PNAS
www.pnas.org

Supplementary Information for

p31^{comet} promotes homologous recombination by inactivating REV7 through the TRIP13 ATPase

Prabha Sarangi*[1], Connor S. Clairmont*[1], Lucas D. Galli[1], Lisa A. Moreau[1], Alan D. D'Andrea[1,2]

1. Department of Radiation Oncology, Dana-Farber Cancer Institute, Boston, MA, 02215, USA
2. Center for DNA Damage and Repair, Dana-Farber Cancer Institute, Boston, MA, 02215, USA

Corresponding Author:

Alan D. D'Andrea, M.D.
Director: Center for DNA Damage and Repair
Harvard Medical School
Department of Radiation Oncology
Dana-Farber Cancer Institute, HIM 243
450 Brookline Ave.
Boston, MA 02215
617-632-2080
FAX: 617-632-6069
Alan_Dandrea@dfci.harvard.edu

This PDF file includes:

Figures S1 to S5

www.pnas.org/cgi/doi/10.1073/pnas.2008830117

Fig S1

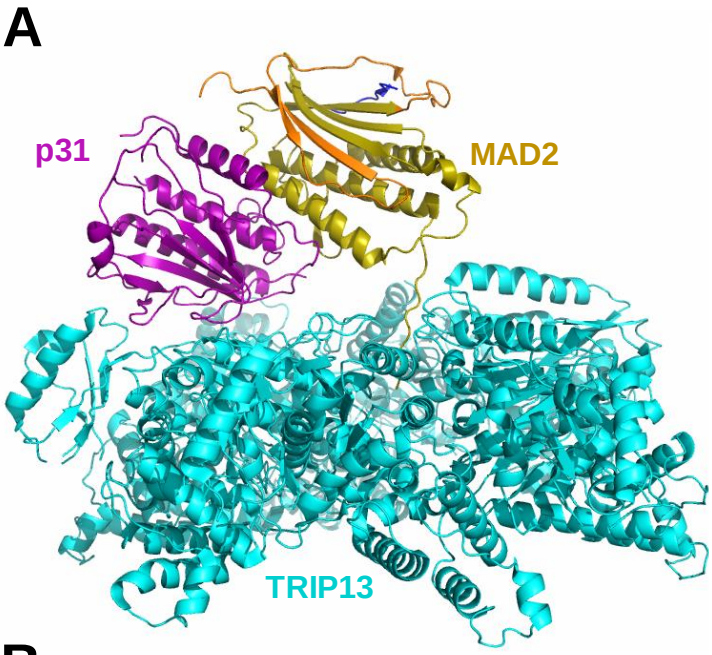

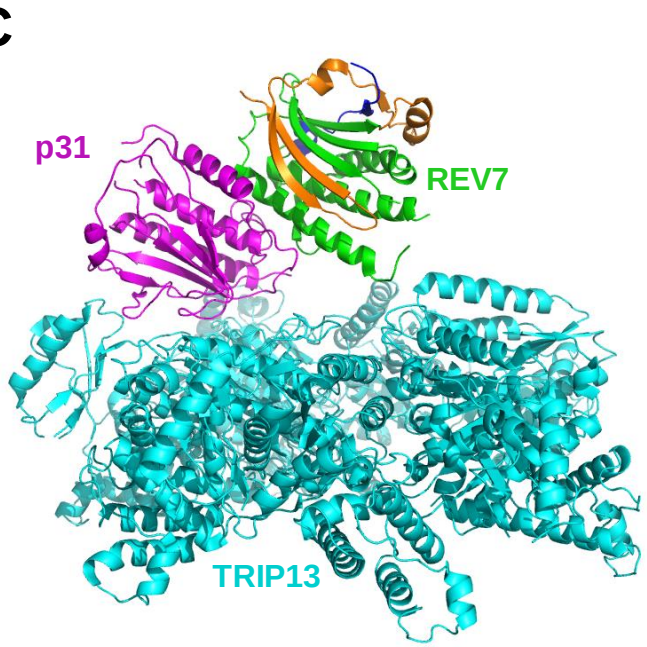

B

```
H._sapiens_REV7      .MTTLTR..QDLNFGQVV...ADVLCEFLEVAVHL
M._musculus_REV7     .MTTLTR..QDLNFGQVV...ADVLSEFLEVAVHL
G._gallus_REV7       .MTTLTR..QDLNFGQVV...ADVLSEFLEVAVHL
X._laevis_REV7       .MTTLTR..QDLNFGQVV...ADILCEFLEVAVHL
H._sapiens_MAD2      MALQLSR...EQ.GIT.LRGSAEIVAEFFSFGINS
M._musculus_MAD2     MAQQLAR...EQ.GIT.LRGSAEIVAEFFSFGINS
G._gallus_MAD2       MAAQLSR...EQQGIT.LRGSAEIVAEFFSYGINS
X._laevis_MAD2       MAGQLTR...E..GIT.LKGSAEIVSEFFFCGINS

Consensus            .Φ.ζLζR...-....ζ.Φ...A-ΦΦ.EFΦ...Φζ.
```

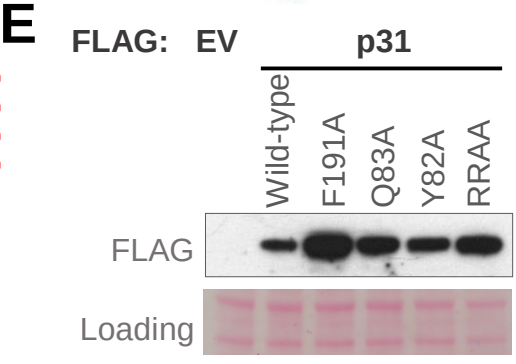

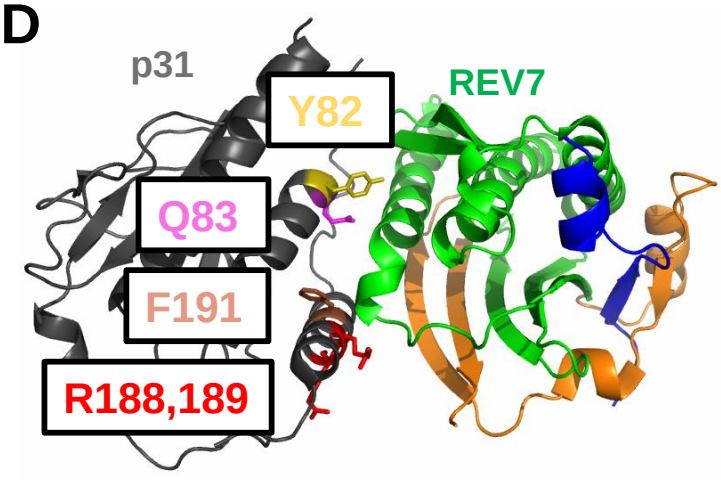

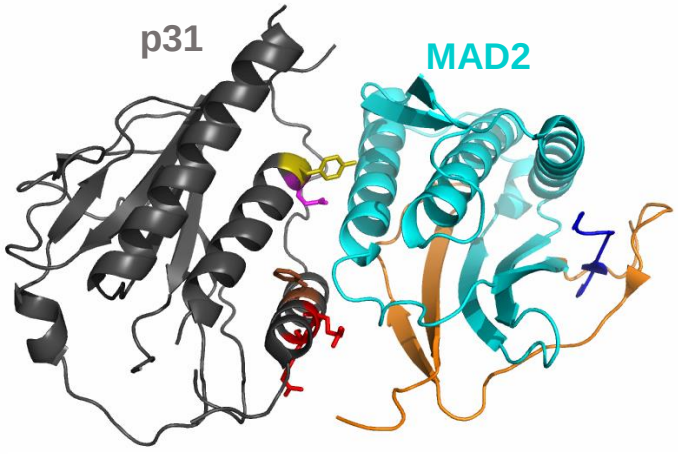

Figure S1: Conservation of p31 and TRIP13 interaction between REV7 and MAD2

(A) Published Cryo-EM structure of the TRIP13-p31-MAD2 complex (PDB: 6F0X). (B) Primary sequence alignment of REV7 and MAD2 from various organisms. The conserved TRIP13 binding motif in REV7 and MAD2 is indicated by the yellow box. In the consensus sequence: red/Φ indicates hydrophobic residues, green/ζ indicates polar residues, pink indicates positively charged residues, blue/- indicates negatively charged residues. (C) Model of REV7-p31-TRIP13 structure based on structural alignment of REV7 (PDB: 3VU7) and MAD2. (D) Reorientation of the published and modelled structures in Figure S1A and S1C to highlight p31 residues predicted to be important for the REV7-p31 interaction. (E) Western blot showing the expression levels of the p31 variants in *p31*$^{-/-}$ HEK293T cells.

Fig S2

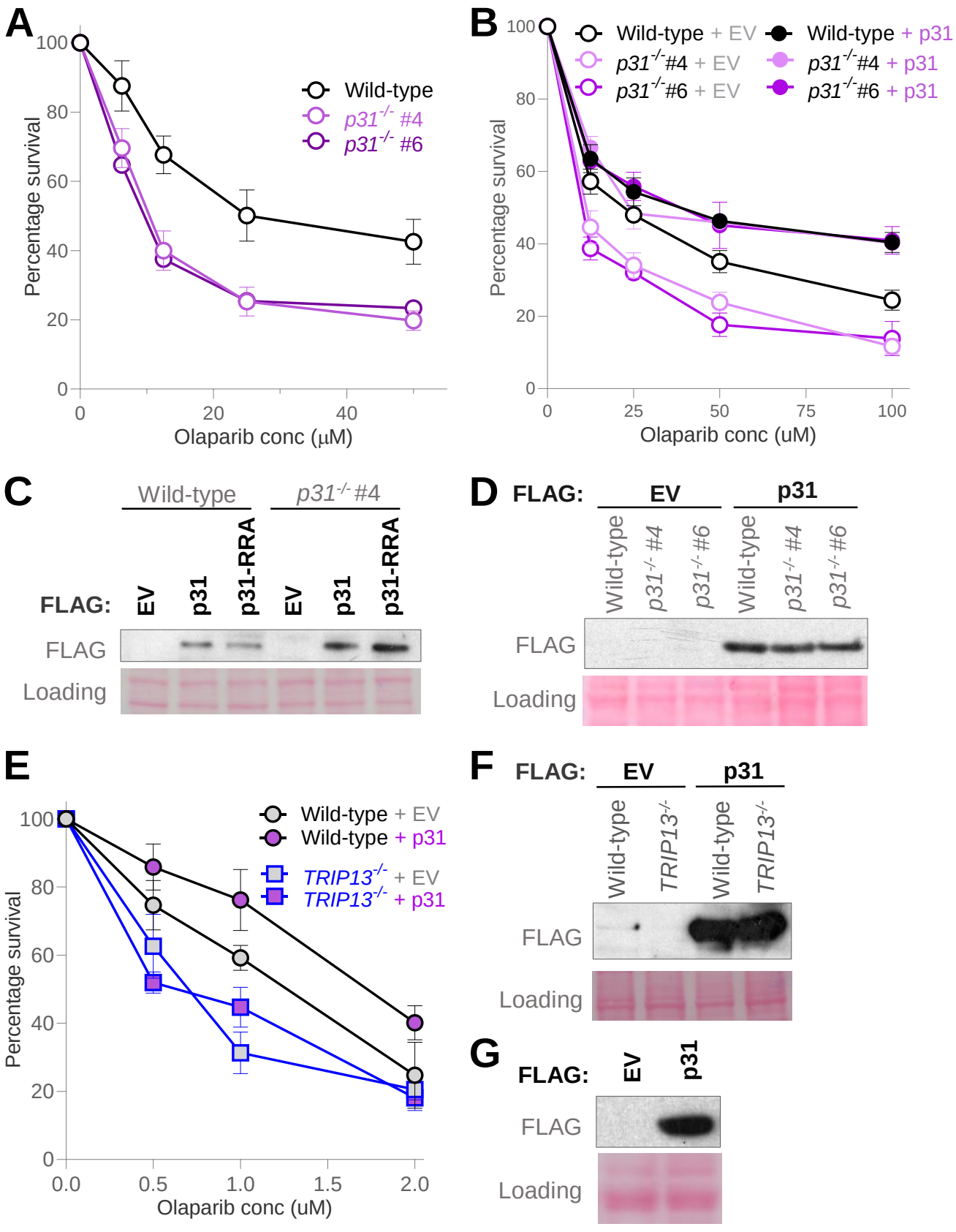
A
Percentage survival
Olaparib conc (μM)
Wild-type
p31-/- #4
p31-/- #6
B
Percentage survival
Olaparib conc (uM)
Wild-type + EV
Wild-type + p31
p31-/-#4 + EV
p31-/-#4 + p31
p31-/-#6 + EV
p31-/-#6 + p31
C
Wild-type
p31-/-#4
FLAG:
EV
p31
p31-RRA
FLAG
Loading
D
FLAG:
EV
p31
Wild-type
p31-/- #4
p31-/- #6
FLAG
Loading
E
Percentage survival
Olaparib conc (uM)
Wild-type + EV
Wild-type + p31
TRIP13-/- + EV
TRIP13-/- + p31
F
FLAG:
EV
p31
Wild-type
TRIP13-/-
FLAG
Loading
G
FLAG:
EV
p31
FLAG
Loading

Figure S2: p31 affects HR proficiency

(A) Short-term cytotoxicity curve of wild-type and two *p31*$^{-/-}$ clones in U2OS cells upon treatment with various doses of Olaparib. Means and standard deviations of 3 independent experiments are depicted. (B) Short-term cytotoxicity curve of wild-type and two *p31*$^{-/-}$ clones in U2OS cells with ectopic expression of empty vector (EV) or wild-type p31 upon treatment with various doses of Olaparib. Means and standard deviations of 3 independent experiments are depicted. (C) Western blot showing the ectopic expression of FLAG-tagged wild-type p31 and RR188,189AA mutant p31 in wild-type and *p31*$^{-/-}$ U2OS cells, related to Figs. 2C-D. (D) Western blot showing the ectopic expression of FLAG-p31, related to Fig. S2B. (E) Clonogenic survival curve of wild-type and *TRIP13*$^{-/-}$ U2OS cells expressing empty-vector (EV) or overexpressing p31, at various doses of Olaparib. Means and standard deviations of 3 independent experiments are depicted. (F) Western blot showing overexpression of p31 in wild-type or *TRIP13*$^{-/-}$ U2OS cells, related to Fig. S2E. (G) Western blot showing overexpression of p31 in *TP53*$^{-/-}$, *BRCA1*$^{-/-}$ RPE-1 cells, related to Fig. 2E.

Fig S3

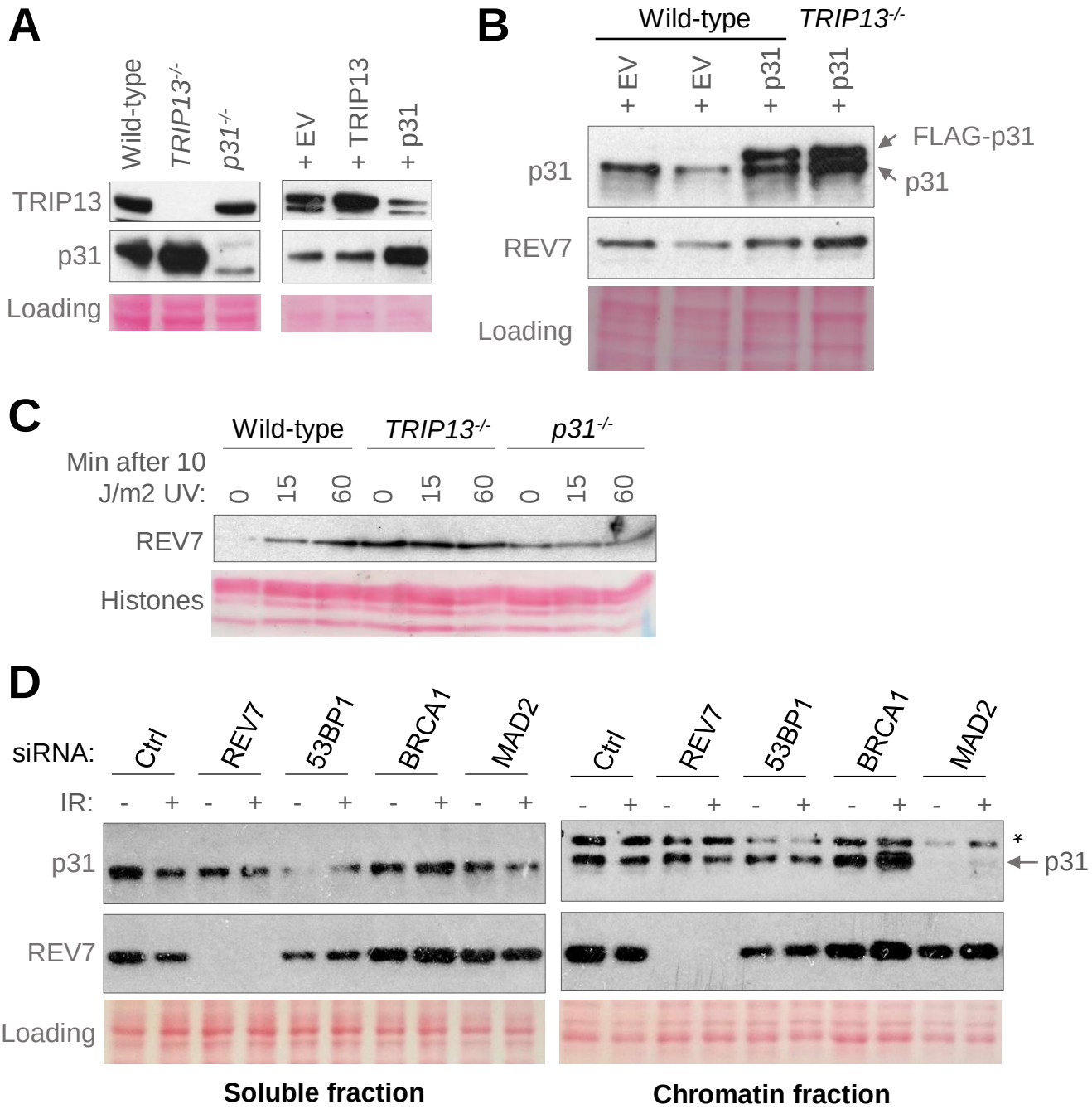
A
Wild-type
TRIP13-/-
p31-/-
+ EV
+ TRIP13
+ p31
TRIP13
p31
Loading
B
Wild-type
TRIP13-/-
+ EV
+ EV
+ p31
+ p31
FLAG-p31
p31
p31
REV7
Loading
C
Wild-type
TRIP13-/-
p31-/-
Min after 10 J/m2 UV:
0
15
60
0
15
60
0
15
60
REV7
Histones
D
siRNA:
Ctrl
REV7
53BP1
BRCA1
MAD2
Ctrl
REV7
53BP1
BRCA1
MAD2
IR:
- + - + - + - + - + - + - + - + - + - +
p31
REV7
Loading
*
p31
Soluble fraction
Chromatin fraction

Figure S3: p31 affects the activation of REV7 in response to damage

(A) Western blot showing the lack of expression of the respective protein in *TRIP13*$^{-/-}$ and *p31*$^{-/-}$ U2OS cells, and overexpression of p31 and TRIP13, related to Figs. 3A-B. (B) Western blot showing the ectopic overexpression of p31 in wild-type and *TRIP13*$^{-/-}$ U2OS cells, related to Fig. 3B-C. (C) Western blot of chromatin bound REV7 from wild-type, *TRIP13*$^{-/-}$, or *p31*$^{-/-}$ U2OS cells following irradiation with 10 J/m^2 of UV light. (D) Western blot showing soluble and chromatin-associated REV7 and p31 following siRNA-mediated knockdown of various proteins. Asterisk denotes non-specific band.

Fig S4

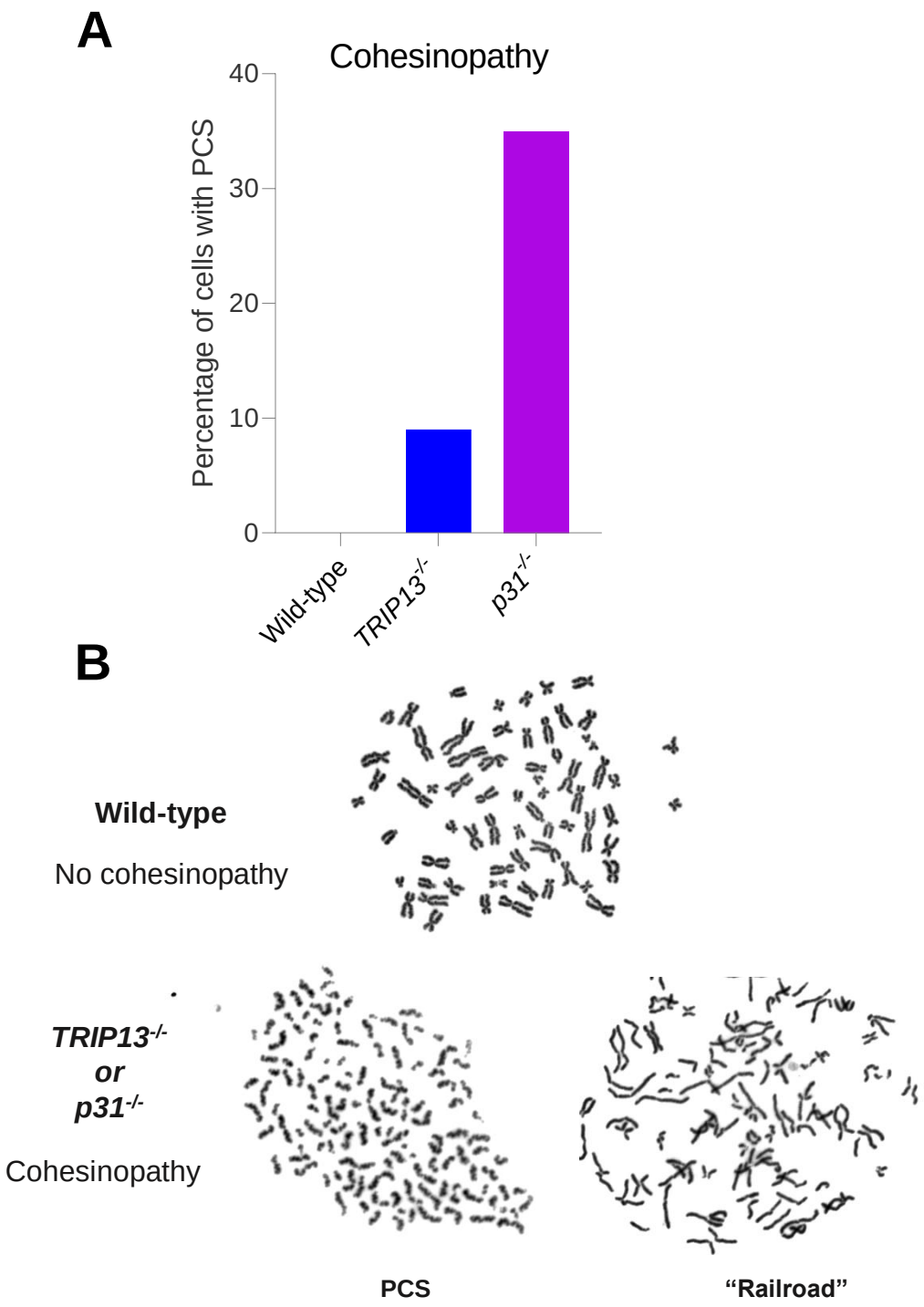
A
Cohesinopathy
Percentage of cells with PCS
40
30
20
10
0
Wild-type
TRIP13-/-
p31-/-
B
Wild-type
No cohesinopathy
TRIP13-/-
or
p31-/-
Cohesinopathy
PCS
"Railroad"

Figure S4: p31 Deficiency Induces Chromosomal Aberrations

(A) Graph showing the prevalence of cohesinopathy observed in metaphase spreads from wild-type, *TRIP13*$^{-/-}$ and *p31*$^{-/-}$ HEK293T cells. (B) Representative images showing cohesinopathy phenotypes quantified in Fig. S4A.

Fig S5

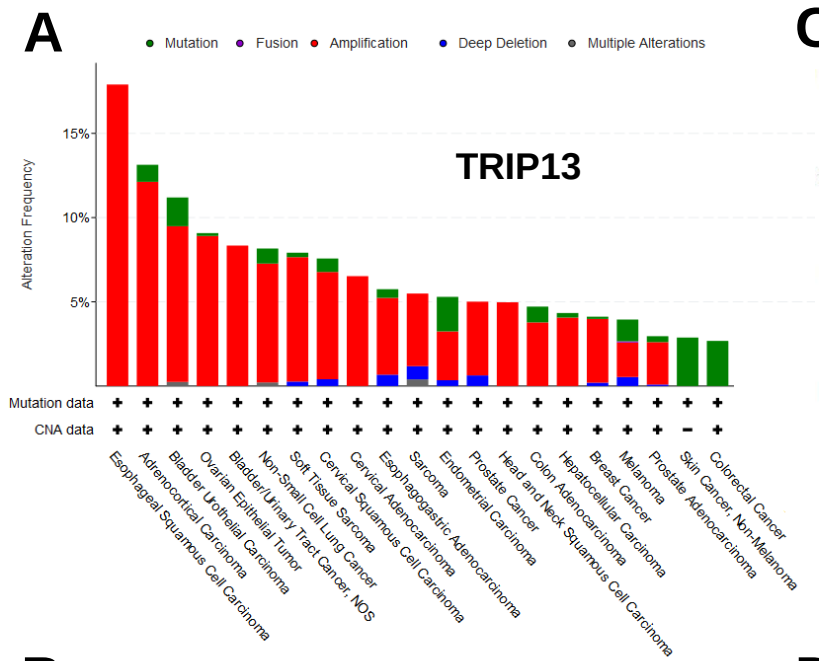
A
Mutation
Fusion
Amplification
Deep Deletion
Multiple Alterations
TRIP13
Alteration Frequency
15%
10%
5%
Mutation data
CNA data
Esophageal Squamous Cell Carcinoma
Adrenocortical Carcinoma
Bladder Urothelial Carcinoma
Ovarian Epithelial Tumor
Bladder/Urinary Tract Cancer, NOS
Non-Small Cell Lung Cancer
Soft Tissue Sarcoma
Cervical Squamous Cell Carcinoma
Cervical Adenocarcinoma
Esophagogastric Adenocarcinoma
Sarcoma
Endometrial Carcinoma
Prostate Cancer
Head and Neck Squamous Cell Carcinoma
Colon Adenocarcinoma
Hepatocellular Carcinoma
Breast Cancer
Melanoma
Prostate Adenocarcinoma
Skin Cancer, Non-Melanoma
Colorectal Cancer

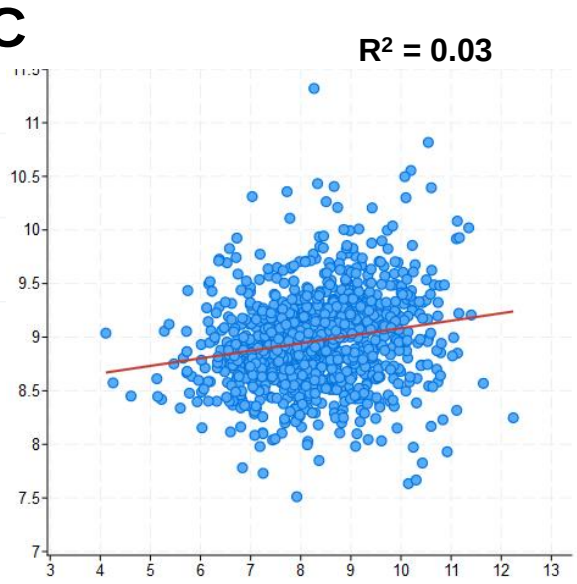
C
R² = 0.03
11
10.5
10
9.5
9
8.5
8
7.5
7
3
4
5
6
7
8
9
10
11
12
13

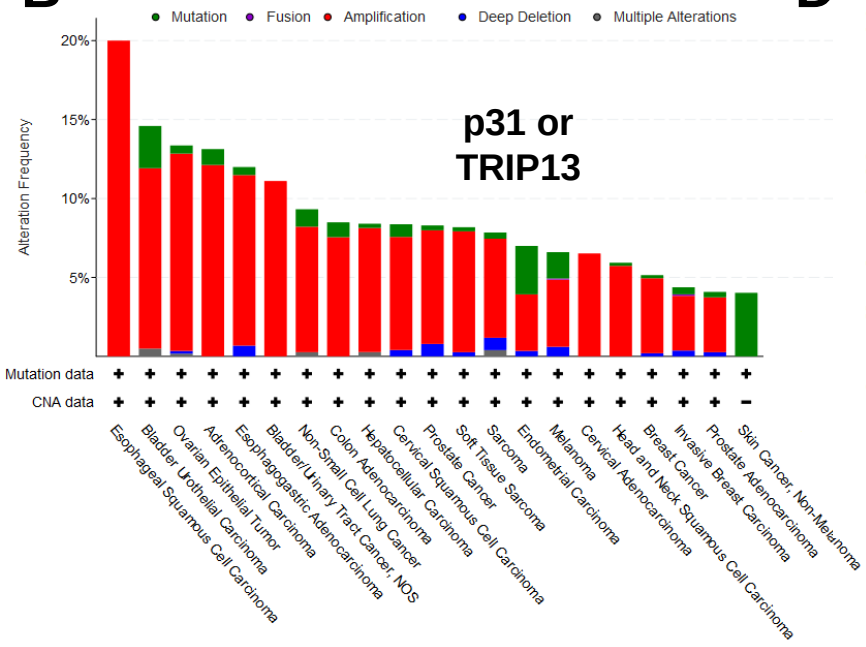
B
Mutation
Fusion
Amplification
Deep Deletion
Multiple Alterations
p31 or TRIP13
Alteration Frequency
20%
15%
10%
5%
Mutation data
CNA data
Esophageal Squamous Cell Carcinoma
Bladder Urothelial Carcinoma
Ovarian Epithelial Tumor
Adrenocortical Carcinoma
Esophagogastric Adenocarcinoma
Bladder/Urinary Tract Cancer, NOS
Non-Small Cell Lung Cancer
Colon Adenocarcinoma
Hepatocellular Carcinoma
Cervical Squamous Cell Carcinoma
Prostate Cancer
Soft Tissue Sarcoma
Sarcoma
Endometrial Carcinoma
Melanoma
Cervical Adenocarcinoma
Head and Neck Squamous Cell Carcinoma
Breast Cancer
Invasive Breast Carcinoma
Prostate Adenocarcinoma
Skin Cancer, Non-Melanoma

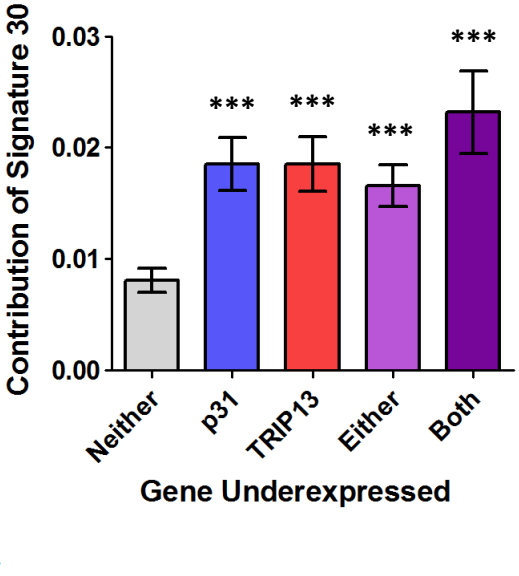
D
Contribution of Signature 30
0.03
0.02
0.01
0.00
***
***
***
***
Neither
p31
TRIP13
Either
Both
Gene Underexpressed

Figure S5: TRIP13 and p31 are independently upregulated in similar cancer types.

(A) Bar chart showing the prevalence of amplifications (red), deletions (blue) and mutations (green) of the TRIP13 gene across an array of cancer types in The Cancer Genome Atlas (TCGA). (B) Similar to Figs. 5A and S5A, showing the prevalence of alterations in either TRIP13 or p31. (C) Scatter plot of TRIP13 expression vs p31 expression in breast cancers, showing no correlation. $R^2 = 0.03$ (Pearson's correlation coefficient). (D) Graph showing the contribution of mutation signature 30 in cancers with low expression of TRIP13 and/or p31 compared to cancers with normal expression of both genes. ***$p<0.001$, Mann-Whitney test, two-tailed.